Analysis of Collaborative Beamforming for Wireless Sensor Networks with Phase Offset

Xiaofeng SHEN[1], Jiyan HUANG[1,3], Peng LIU[2], Yijiang PAN[1], Baogen XU[3], Zhongchu RAO[3]

[1]Dept. of Electronic Engineering, University of Electronic Science and Technology of China, Chengdu, China
[2] The Academy of Satellite Application, BeiJing, China
[3]Tong Fang Electronic Technology Company Limited, Jiangxi, China

huangjiyan@uestc.edu.cn

Abstract. *Collaborative beamforming has been widely used in wireless sensor networks to improve the directivity of signals in long-distance transmission. The performance of collaborative beamforming has been well analyzed for the case without phase offset in the literature. However, the phase ambiguity caused by carrier phase jitter or offset between the transmitter and receiver nodes always exists in a practical system. Although the effects of imperfect phase have been studied for uniform node distribution and Tikhonov phase noise model, the performance analysis of collaborative beamforming with arbitrary node distributions and any phase offset which may have various probability density functions (PDFs) depending on phase-locked loop circuits is still an open issue. This paper proposes a unified method to evaluate the performance of collaborative beamforming in the case of phase noise. Since non-parametric kernel method is used to build the PDFs of node and phase offset, the proposed non-parametric approach can provide accurate performance analysis for various node and phase noise distributions which may or may not be represented by explicit PDF functions. Computer simulation is conducted to verify validity of the proposed method.*

Keywords

Collaborative beamforming, wireless sensor networks, kernel method, node distributions, phase offset, performance analysis.

1. Introduction

Wireless sensor networks (WSNs) are widely used for monitoring and control in military, environmental, health and commercial systems [1]. A WSN usually consists of hundreds of small, battery-powered and wirelessly connected sensors. Each sensor in a WSN usually has limited communication range due to cost and resource constraints. A preferred solution to increase communication range and save transmission energy is the distributed or collaborative beamforming. Collaborative beamforming is achieved by adjusting the initial phase of each node to form a beam in the desired direction as shown in Fig. 1. Therefore, interference at other directions is suppressed and signal at the receiver becomes dominant.

Several collaborative beamforming methods have been investigated in the literature [2–5]. However, the characteristics of beampatterns were seldom studied. The authors in [6] analyzed the performance of collaborative beamforming using the random array theory developed in [7] based on the assumption that sensor nodes are uniformly distributed in a WSN. Furthermore, the effects of imperfect phase have been studied in [6] when the positions of nodes follow a uniform distribution and phase noise is subject to Tikhonov distribution. In a large WSN, when sensor nodes drop from an airplane for example, the positions of nodes are affected by many factors such as wind speed and direction, sensor releasing mechanism, and height of releasing point. According to the central limit theorem, the combined effect of these factors results in Gaussian node distribution. Therefore, the beampattern characteristics for the Gaussian node distribution in [8] provided a unified performance analysis for large WSNs. The total effect of these factors may change in small WSNs. In this case, node distribution may not be described by Gaussian distribution. To present a unified analysis of collaborative beamforming for arbitrary node distributions and any size of WSNs, a non-parametric method was proposed to evaluate the performance of collaborative beamforming in [9].

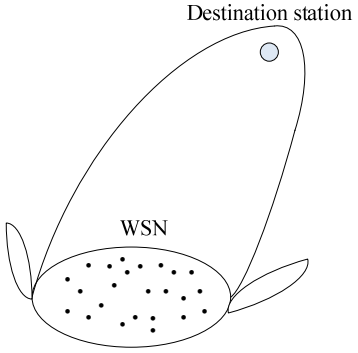

Fig. 1. Collaborative beamforming in WSNs.

It should be noted that the effects of imperfect phase was only studied for the case that the positions of nodes follow a uniform distribution and the phase offset is subject to Tikhonov distribution whereas both [8] and [9] do not take the phase offset into consideration. Therefore, the performance analysis of collaborative beamforming with arbitrary node distributions and any phase offset which may have various distributions depended on phase-locked loop (PLL) circuits is still an open issue. This paper presents analysis of collaborative beamforming for the case of imperfect phase synchronization. The basic idea of the proposed method is to model the probability density functions (PDFs) of node and phase offset distributions using the non-parametric kernel method and then derive the beampattern properties based on the estimated PDFs. The non-parametric kernel method is an attractive and powerful tool to estimate the PDF of an actual distribution from survey data and has a wide range of applications in machine learning, bioinformatics, and computer vision [10]. Since kernel density estimators asymptotically converge to any PDF, the application of kernel density estimation enables the proposed method to be independent from the assumptions of the underlying node and phase noise distributions.

2. System Description

Considering a geometric model in [6], [8–9] with N sensor nodes, the Cartesian coordinates of the k^{th} sensor node are denoted by (x_k, y_k). The corresponding spherical coordinates are $\left(r_k=\sqrt{x_k^2+y_k^2},\psi_k=\tan^{-1}\left(\frac{y_k}{x_k}\right)\right)$. The location vectors $\mathbf{r}$ and $\boldsymbol{\psi}$ for all nodes can be written as:

$$\begin{aligned}\mathbf{r}&=\left[r_1,r_2,\cdots,r_N\right]\in\left[0,\infty\right)^N\\ \boldsymbol{\psi}&=\left[\psi_1,\psi_2,\cdots,\psi_N\right]\in\left[-\pi,\pi\right)^N\end{aligned}\tag{1}$$

Since collaborative beamforming is generally used for long-distance transmission, this paper focuses on the radiation pattern in the far-field region. Assuming that the position of the destination base station is (A,ϕ_0) in spherical coordinates, performance analysis for collaborative beamforming is to obtain the characteristics of beampatterns at the point (A,ϕ) where $\phi\in[-\pi,\pi)$. The wavelength of signal is λ. The distance between the k^{th} sensor node and point (A,ϕ) is:

$$\begin{aligned}d_k(\phi)&=\sqrt{A^2+r_k^2-2r_kA\cos(\phi-\psi_k)}\\&\approx A-r_k\cos(\phi-\psi_k)\end{aligned}\tag{2}$$

where $A>>r_k$ in the far-field region.

To form a beam at the desired direction (A,ϕ_0) for long-distance and high-speed transmission, the initial phase of node k should be synchronized as:

$$\psi_k=-\tfrac{2\pi}{\lambda}d_k(\phi_0)\tag{3}$$

where $d_k(\phi_0)$ is the distance between the k^{th} sensor node and destination base station (A,ϕ_0). Due to the phase ambiguity caused by carrier phase jitter or offset between the transmitter and receiver nodes, the initial phase of node k becomes:

$$\bar{\psi}_k=-\tfrac{2\pi}{\lambda}d_k(\phi_0)+\varphi_k\tag{4}$$

where φ_k corresponds to the phase offset and is assumed to be an i.i.d. random variable. The corresponding array factor, given the realizations of node locations $(\mathbf{r},\boldsymbol{\psi})$ and phase offset $\boldsymbol{\varphi}$, is written as:

$$\begin{aligned}F(\phi\,|\,\mathbf{r},\boldsymbol{\psi},\boldsymbol{\varphi})&=\frac{1}{N}\sum_{k=1}^{N}e^{j\bar{\psi}_k}e^{j\frac{2\pi}{\lambda}d_k(\phi)}\\&\approx\frac{1}{N}\sum_{k=1}^{N}e^{j\frac{2\pi}{\lambda}r_k\left(\cos(\phi_0-\phi_k)-\cos(\phi-\phi_k)\right)}e^{j\varphi_k}\\&=\frac{1}{N}\sum_{k=1}^{N}e^{j\frac{4\pi}{\lambda}r_k\sin\left(\phi_k-\frac{\phi_0+\phi}{2}\right)\sin\left(\frac{\phi_0-\phi}{2}\right)}e^{j\varphi_k}\end{aligned}\tag{5}$$

where $\boldsymbol{\varphi}=\left[\varphi_1,\cdots,\varphi_N\right]^T$. Without loss of generality, the azimuth direction of the destination base station ϕ_0 is assumed to be 0 and the array factor is given by:

$$\begin{aligned}F(\phi\,|\,\mathbf{z},\boldsymbol{\varphi})&=\frac{1}{N}\sum_{k=1}^{N}e^{-j\frac{4\pi}{\lambda}r_k\sin(\phi_k-\phi/2)\sin(\phi/2)}e^{j\varphi_k}\\&=\frac{1}{N}\sum_{k=1}^{N}e^{-jaz_k}e^{j\varphi_k}\end{aligned}\tag{6}$$

where $a=a(\phi)=4\pi\sin\left(\frac{\phi}{2}\right)$, $\mathbf{z}=\left[z_1,z_2,\cdots,z_N\right]\in\left(-\infty,+\infty\right)^N$, and $z_k=\frac{r_k}{\lambda}\sin\left(\psi_k-\frac{\phi}{2}\right)$. Since z_k is related to the spherical coordinates (r_k,ψ_k) of node k and the sensors in WSNs are usually randomly and densely deployed in a certain area, z_k is a random variable which may have different PDFs depending on the deployment methods and environments. Phase offset also has various distributions caused by different PLL circuits.

The far-field beampattern can be defined as:

$$\begin{aligned}P(\phi\,|\,\mathbf{z},\boldsymbol{\varphi})&=\left|F(\phi\,|\,\mathbf{z},\boldsymbol{\varphi})\right|^2\\&=F(\phi\,|\,\mathbf{z},\boldsymbol{\varphi})F^*(\phi\,|\,\mathbf{z},\boldsymbol{\varphi})\\&=\frac{1}{N^2}\sum_{k=1}^{N}e^{-jaz_k}e^{j\varphi_k}\sum_{l=1}^{N}e^{jaz_l}e^{-j\varphi_l}\\&=\frac{1}{N}+\frac{1}{N^2}\sum_{k=1}^{N}e^{-jaz_k}e^{j\varphi_k}\sum_{l=1,l\neq k}^{N}e^{jaz_l}e^{-j\varphi_l}\end{aligned}\tag{7}$$

Beampattern describes the array gains in the whole region $\phi \in [-\pi, \pi)$. The objective of collaborative beamforming is to enhance the array gain at the direction of destination and suppress the gains at other directions. Since $P(\phi \mid \mathbf{z}, \boldsymbol{\varphi})$ contains the random variable z_k and φ_k, the characteristics of beampatterns should be derived in statistical sense.

3. Average Characteristics of Beampattern

Since the performance of collaborative beamforming depends on distributions of the sensor node and phase offset, the PDFs of z_k and φ_k should be calculated. There are parametric and non-parametric methods for estimating the PDFs of z_k and φ_k. The parametric methods can only be used for specific node distributions such as uniform and Gaussian distributions in [6], [8]. In Sections 3 and 4, a non-parametric method is developed to evaluate the performance of collaborative beamforming for all nodes and phase offset distributions with or without explicit PDFs.

The basic procedure of non-parametric estimation is to create an approximation of the PDF from a set of survey measurements (or called sample points). Assuming that the survey set $\{\bar{z}_1, \bar{z}_2, \cdots, \bar{z}_M\}$ with size M is available for z_k, the estimated PDF of z_k can be obtained using non-parametric Gaussian kernel method [10], [11]:

$$f_{z_k}(z) = \frac{1}{\sqrt{2\pi}Mh} \sum_{t=1}^{M} \exp\left(-\frac{(z - \bar{z}_t)^2}{2h^2} \right) \tag{8}$$

where exp(•) is the Gaussian kernel function and the smoothing constant h is the width of kernel function which can be determined by Expectation–maximization (EM) method in [10], [11]. It should be noted that the non-parametric method (8) is a one-dimensional Gaussian Mixture Model (GMM). Many non-parametric estimators such as histogram method, orthogonal series, and other kernel methods can effectively estimate the PDF and have the similar performance. Gaussian kernel method was chosen due to its similarity with the Euclidean distance and its better smoothing and continuous properties even with a small number of samples [11]. Another reason is that it is easy to integrate and differentiate and can lead to mathematically tractable solution.

Broadly, there are two ways to obtain sample points: empirical model and field measurements. Take node model as an example, different deployment methods and environments will lead to various node distributions. Several distributions with or without explicit PDFs (uniform [6], Gaussian [8], and differential [12]) have been proposed to describe the distribution of sensor nodes in a WSN. For empirical model with explicit PDFs such as uniform and Gaussian distributions, numerical methods [13], [14] or Matlab functions such as "rand" and "normrnd" can be used to generate random variables which follow the desired PDF. These random variables are used as sample points. For empirical model without explicit PDF such as Differential distribution, sample points can also be generated through computer simulations which follow the special deploy methods. The deploy method of Differential distribution will be presented in Section 5. For the case without the prior information on empirical model, field measurement is a useful method to obtain sample points. If both empirical model and field measurements are not available, the problem of performance analysis of Collaborative Beamforming for WSNs will become unsolvable.

Similarly, the estimated PDF of φ_k can be modeled as:

$$f_{\varphi_k}(\varphi) = \frac{1}{\sqrt{2\pi}Ls} \sum_{t=1}^{L} \exp\left(-\frac{(\varphi - \bar{\varphi}_t)^2}{2s^2} \right) \tag{9}$$

where $\{\bar{\varphi}_1, \bar{\varphi}_2, \cdots, \bar{\varphi}_L\}$ with size L is the survey set for φ_k. The minimum values of M and L for achieving relatively accurate results using the kernel method can be determined using the method in [9].

3.1 Average Beampattern

The average beampattern of $\mathbf{z}$ and $\boldsymbol{\varphi}$ is defined as:

$$P_{av}(\phi) = E_{\mathbf{z},\boldsymbol{\varphi}} \{ P(\phi \mid \mathbf{z}, \boldsymbol{\varphi}) \} \tag{10}$$

It can be seen from Appendix A that the average beampattern is derived as:

$$P_{av}(\phi) = \frac{1}{N} + \left(1 - \frac{1}{N}\right) |A_\varphi|^2 |A_z|^2 \tag{11}$$

where $A_\varphi = \frac{1}{L} \sum_{t=1}^{L} e^{j\bar{\varphi}_t}$, and $A_z = \frac{1}{M} \sum_{t=1}^{M} e^{-ja\bar{z}_t}$. Term $1/N$ in (11) is the average power level of the sidelobe. The second term represents the average beampattern of the mainlobe, which depends on the node location, the spatial distribution of the sensor nodes and the phase offset A_ϕ. Different spatial distributions will lead to different waves of $P_{av}(\phi)$. The uniform distribution assumption results in nulls and sidelobes, whereas the average beampattern based on Gaussian distribution has no nulls.

In the case of perfect phase synchronization $\bar{\varphi}_t = 0$ ($t = 1, \cdots, L$), $P_{av}(\phi)$ becomes:

$$\begin{aligned} P_{av}(\phi) &= \frac{1}{N} + \left(1 - \frac{1}{N}\right) |A_z|^2 \\ &= \frac{1}{N} + \left| \frac{1}{M} \sum_{t=1}^{M} e^{-ja\bar{z}_t} \right|^2 \left(1 - \frac{1}{N}\right) \end{aligned} \tag{12}$$

Note that (12) is the average beampattern derived for the case without phase offset in [9]. Thus the proposed average beampattern (11) for the case with phase noise reduces to that of the case without phase offset when phase offset tends to 0. Since $|A_\phi| \le 1$, the phase offset A_ϕ will degrade the array gains in the whole region $\phi \in [-\pi, \pi)$. Therefore $|A_\phi|^2$ is called as degradation factor. This implies that accurate phase synchronization will increase array gain at the desired direction.

It should be noted that (11) and (12) provide approximations of the average beampatterns from a set of survey measurements for the cases with or without phase noise, respectively. It is important to analyze the relationship between the proposed average beampattern and the average beampatterns for uniform [6] and Gaussian [8] node cases. It has been shown in Appendix B that the average beampattern derived using the proposed method becomes Gaussian [8] or uniform [6] average beampattern when the nodes are subject to corresponding distribution and phase offset tends to 0. This gives a sanity check for the proposed method.

3.2 3dB Beamwidth

The 3dB beamwidth is defined as the angle ϕ_{3dB} at which the power of the average beampattern drops 3 dB below its maximum value at $\phi = 0$ [6], [8]:

$$P_{av}\left(\phi_{3dB}\right) = 1/2, N \to \infty . \tag{13}$$

ϕ_{3dB} describes the width of mainlobe. Generally, a sharp mainbeam property is desirable for collaborative beamforming. Substituting (11) into (13) yields:

$$\frac{|A_\varphi|}{M}\left|\sum_{t=1}^{M} e^{-ja(\phi_{3dB})\bar{z}_t}\right| = \frac{1}{\sqrt{2}} . \tag{14}$$

Several numerical methods such as Matlab function "fsolve" can be used to calculate $a(\phi_{3dB})$. After solving $a(\phi_{3dB})$, ϕ_{3dB} can be obtained:

$$\phi_{3dB} = 2\arcsin\left(\frac{a\left(\phi_{3dB}\right)}{4\pi}\right). \tag{15}$$

3.3 3dB Sidelobe Region

The 3dB sidelobe region is defined as the range between the angle $\phi_{sidelobe}$ and π as follows: Sidelobe Region = $\{\phi \mid \phi_{sidelobe} \le \phi \le \pi\}$ [8]. Two examples of the 3dB sidelobe region for uniform and Gaussian node distributions are shown in Fig. 2. The 3 dB sidelobe region is used to show the region within which the average of the sidelobe beampattern falls between $1/N$ and $2/N$. Since the dominant nonnegligible sidelobe peaks are within the range between ϕ_{3dB} and $\phi_{sidelobe}$, larger $\phi_{sidelobe}$ will lead to stronger interference at the undesired directions. The angle $\phi_{sidelobe}$ should satisfy [8]:

$$P_{av}\left(\phi_{sidelobe}\right) = \frac{2}{N} . \tag{16}$$

It should be noted that there may be several solutions for (16). To make sure that the average of the sidelobe beampattern falls below $2/N$, the maximum value of the solutions will be chosen as $\phi_{sidelobe}$. The steps to obtain $\phi_{sidelobe}$ are listed here:

(1) Set $\phi = [1°, 1.1°, \ldots, 180°]$.

(2) Substitute ϕ_i into (16) and calculate $error(i) = P_{av}(\phi_i) - 2/N$.

(3) If $error(i-1) \cdot error(i+1) < 0$, then record $\phi'_j = \phi_i$.

(4) Finally get $\phi_{sidelobe} = \max(\phi'_j)$.

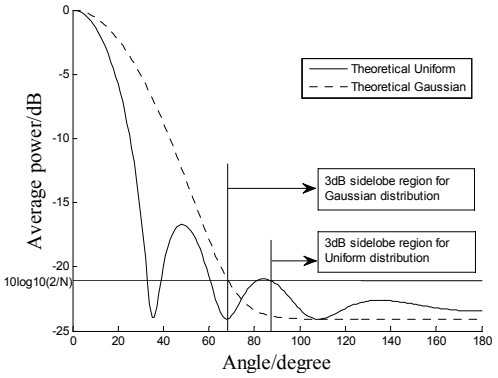

Fig. 2. Definition of 3dB sidelobe region.

3.4 Average Directivity

The directivity is used to describe how much radiated energy is contained at the desired direction, which is defined as:

$$D(\mathbf{z}) = \frac{\int_{-\pi}^{\pi} P(0 \mid \mathbf{z}, \boldsymbol{\varphi}) d\phi}{\int_{-\pi}^{\pi} P(\phi \mid \mathbf{z}, \boldsymbol{\varphi}) d\phi} . \tag{17}$$

Then, the average directivity is defined as $D_{av} = E_{z,\phi}[D(\mathbf{z})]$. Furthermore, the lower bound of D_{av} can be obtained as:

$$D_{av}^{*} = \frac{\int_{-\pi}^{\pi} P_{av}(0) d\phi}{\int_{-\pi}^{\pi} P_{av}(\phi) d\phi} . \tag{18}$$

Substituting (11) into (18) gives:

$$\begin{aligned} D_{av}^{*} &= \frac{2\pi\left(\frac{1}{N} + \left(1 - \frac{1}{N}\right)|A_\varphi|^2\right)}{\int_{-\pi}^{\pi}\left(\frac{1}{N} + \left(1-\frac{1}{N}\right)|A_\varphi|^2\left(\left|\frac{1}{M}\sum_{t=1}^{M} e^{-ja\bar{z}_t}\right|^2\right)\right) d\phi} \\ &= \frac{2\pi\left(1 + (N-1)|A_\varphi|^2\right)}{2\pi + (N-1)|A_\varphi|^2 \int_{-\pi}^{\pi}\left|\frac{1}{M}\sum_{t=1}^{M} e^{-ja\bar{z}_t}\right|^2 d\phi} \end{aligned} . \tag{19}$$

The normalized directivity is defined as:

$$\tilde{D}_{av} = D_{av}^{*} / N . \tag{20}$$

4. Random Characteristics of Beampattern

The properties of the average beanpattern are derived in Section 3. This section presents analysis for the statistical distribution of beampattern for arbitrary node and phase offset distributions using the proposed non-parametric method. The array factor of (6) can be rewritten as [6]:

$$F(\phi \mid \mathbf{z}) = \frac{1}{\sqrt{N}}(X - jY) \tag{21}$$

where

$X = \frac{1}{\sqrt{N}}\sum_{k=1}^{N}\cos(az_k - \varphi_k)$ and $Y = \frac{1}{\sqrt{N}}\sum_{k=1}^{N}\sin(az_k - \varphi_k)$.

The distribution of the array factor is approximated by the complex Gaussian distribution in [6], [8], its PDF is:

$$f_{X,Y}(x,y) = \frac{1}{2\pi\sigma_x\sigma_y}\exp\left[-\frac{|x-m_x|^2}{2\sigma_x^2} - \frac{|y-m_y|^2}{2\sigma_y^2}\right] \tag{22}$$

where m_x, σ_x^2, m_y, and σ_y^2 are the means and variances of X and Y, respectively. The complementary cumulative distribution function (CCDF) of a beampattern, which is defined as the probability that the radiated power density in the direction of ϕ exceeds a threshold power, is given by [9]:

$$\begin{aligned}&\Pr\left[P(\phi) > P_0\right] = \iint_{x^2+y^2>NP_0} f_{X,Y}(x,y)\,dxdy \\ &= \int_{-\pi}^{+\pi}\frac{e^{-W_w}}{4\pi\sigma_x\sigma_y U_w^2}\left\{\sqrt{\pi}V_w erfc\left(U_w\sqrt{NP_0} - V_w\right) + e^{-\left(U_w\sqrt{NP_0}-V_w\right)^2}\right\}dw\end{aligned} \tag{23}$$

where

$$U_w = \sqrt{\frac{\cos^2 w}{2\sigma_x^2} + \frac{\sin^2 w}{2\sigma_y^2}},$$

$$V_w = \frac{\sigma_y^2 m_x \cos w + \sigma_x^2 m_y \sin w}{2\sigma_x^2\sigma_y^2 U_w},$$

$$W_w = \frac{m_x^2}{2\sigma_x^2} + \frac{m_y^2}{2\sigma_y^2} - V_w^2 .$$

To make the CCDF solvable, m_x, σ_x^2, m_y, and σ_y^2 should be calculated first. Since z_k and φ_k are independent, the joint PDF for these two variables can be obtained from (8) and (9):

$$f_k(z,\varphi) = \frac{1}{2\pi MhLs}\sum_{t=1}^{M}\exp\left(-\frac{(z-\bar{z}_t)^2}{2h^2}\right)\sum_{t=1}^{L}\exp\left(-\frac{(\varphi-\bar{\varphi}_t)^2}{2s^2}\right). \tag{24}$$

From (21) and (24), the means and variances of X and Y are derived as:

$$\begin{aligned}
&m_x = E[X] = \int_{-\infty}^{+\infty}\int_{-\infty}^{+\infty}\frac{1}{\sqrt{N}}\sum_{k=1}^{N}\cos(az_k - \varphi_k) f_k(z,\varphi)dz_k d\varphi_k \\
&\sigma_x^2 = Var[X] \\
&= \int_{-\infty}^{+\infty}\int_{-\infty}^{+\infty}\left(\frac{1}{\sqrt{N}}\sum_{k=1}^{N}\cos(az_k - \varphi_k)\right)^2 f_k(z,\varphi)dz_k d\varphi_k - m_x^2 \\
&m_y = E[Y] = \int_{-\infty}^{+\infty}\int_{-\infty}^{+\infty}\frac{1}{\sqrt{N}}\sum_{k=1}^{N}\sin(az_k - \varphi_k) f_k(z,\varphi)dz_k d\varphi_k \\
&\sigma_y^2 = Var[Y] \\
&= \int_{-\infty}^{+\infty}\int_{-\infty}^{+\infty}\left(\frac{1}{\sqrt{N}}\sum_{k=1}^{N}\sin(az_k - \varphi_k)\right)^2 f_k(z,\varphi)dz_k d\varphi_k - m_y^2
\end{aligned} \tag{25}$$

Several numerical methods such as Matlab function "dblquad" can be used to calculate the above quantities.

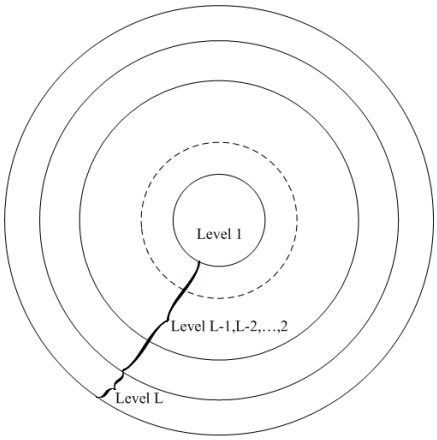

Fig. 3. Differential deployment Method in [12].

5. Simulation Results

Both uniform and Gaussian distributions in [6] and [8] are selected to validate the proposed method for explicit node distribution functions. The differential distribution in [12] is chosen to simulate inexplicit node distributions in practical WSNs. To deploy the differential node distribution [12], it is assumed that the network covers a disk area divided into L levels from the center to the outside as shown in Fig. 3. Each level has same length but different node densities. Nodes are randomly and uniformly distributed in each level. L is set to 5 and node probability densities for levels 1 to 5 are 29.55 %, 27.18 %, 22.41 %, 15.23 %, and 5.63 % respectively [12]. Node probability density shows the percent of sensors located at each level. Therefore the PDF of differential distribution cannot be represented by an explicit expression. The number of sensor nodes is $N = 16$. To compare the three distributions under the same coverage area of the sensor nodes, the normalized radius $\tilde{R} = R/\lambda$ of uniform and differential distributions is set to 3σ [8]. σ is the standard deviation of the Gaussian distribution. R is the radius of the disk. In this case, both uniform and differential distributions have the

same radius $\tilde{R}$ and 99.73 % of all sensor nodes are located in the disk of radius $\tilde{R}$ for Gaussian distribution.

A typical phase jitter model for PLL circuits, which assumes that the phase offset has a Tikhonov distribution, is used to generate the phase noise:

$$f_{\varphi}(x) = \frac{1}{2\pi I_0\left(\frac{1}{\sigma_{\varphi}^2}\right)} \exp\left(\frac{\cos(x)}{\sigma_{\varphi}^2}\right) \tag{26}$$

where σ_{φ}^2 is the variance of the phase noise, and $I_n(x)$ is the n^{th}-order modified Bessel function of the first kind. This phase model was also used in [6] to simulate the phase offset. The variance of phase noise σ_{φ}^2 is related to the loop Signal-Noise-Ratio (SNR) of the PLL by:

$$\rho_{\varphi} = \frac{1}{\sigma_{\varphi}^2}. \tag{27}$$

The corresponding degradation factor derived from (26) is given by [6]:

$$\left|A_{\varphi}\right|^2 = \left(I_1\left(\frac{1}{\sigma_{\varphi}^2}\right) / I_0\left(\frac{1}{\sigma_{\varphi}^2}\right)\right)^2. \tag{28}$$

5.1 Modeling the Degradation Factor by Kernel Method

This experiment is to evaluate the non-parametric kernel method for estimating the degradation factor $|A_{\phi}|^2$ of phase noise from survey data. Phase noise is modeled as Tikhonov random variable, and its theoretical degradation factor $A_{\phi}|^2$ can be obtained from (28). The theoretical and estimated degradation factors of the Tikhonov distribution with different loop SNRs using the theoretical degradation factor (28) and estimated degradation factor (33) are plotted in Fig. 4. It can be seen that the theoretical and estimated degradation factors are basically the same with different loop SNRs. Fig. 4 shows that the proposed equation for degradation factor estimation (33) is effective.

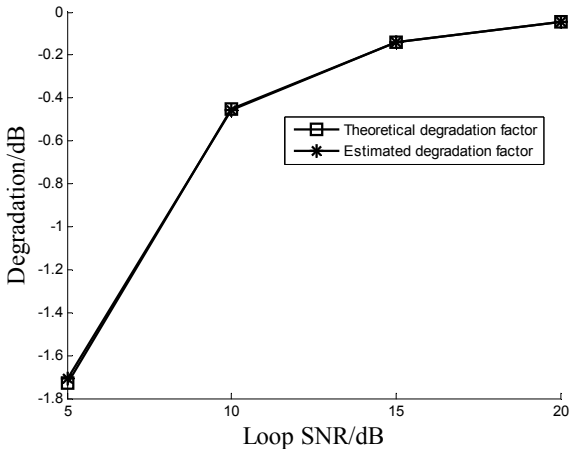

Fig. 4. Degradation factor comparison.

5.2 Characteristics of Beampatten

Since the effective of the non-parametric method to evaluate the performance of collaborative beamforming with perfect phase synchronization for different node distributions has been verified in [9], this paper focuses on analysis of effects of the phase noise applied in beampattern properties.

This simulation is conducted to compare the beampattern characteristics of three node distributions between the cases with or without phase noise. The beampattern characteristics of uniform, Gaussian, and differential distributions for the case without phase noise are obtained from [6], [8], and [9], respectively, while the proposed method is used to analyze the performance of the cases that phase synchronization is imperfect. In order to compare the proposed method with the method considering phase noise, theoretical values [6] including average beampattern, 3dB width, 3dB sidelobe region, and normalized directivity derived for the case of uniform node distribution and Tikhonov phase noise model are also added in the simulation. The performance analysis of CCDF for this case is not provided in [6]. The average beampatterns of three distributions are shown in Figs. 5-7 respectively.

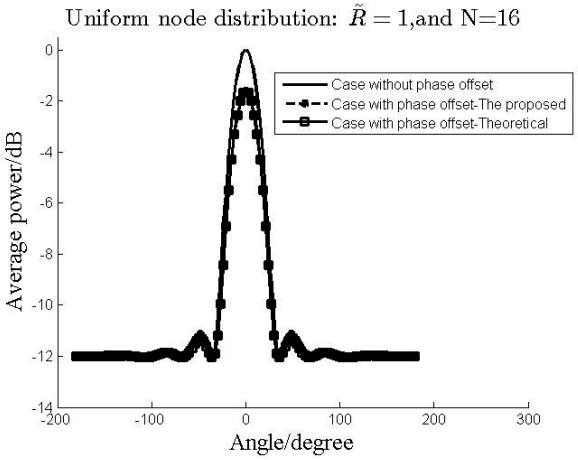

Fig. 5. Average beampattern comparison for uniform node distribution.

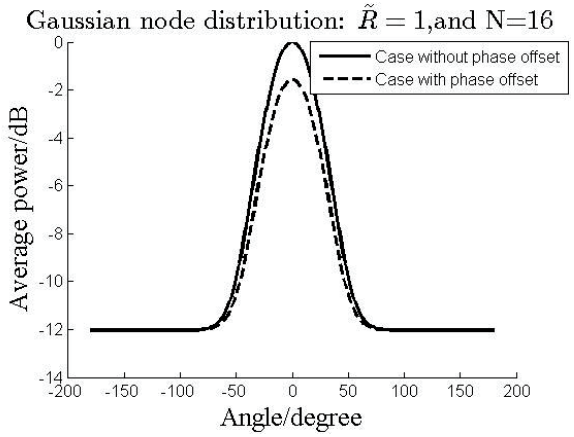

Fig. 6. Average beampattern comparison for Gaussian node distribution.

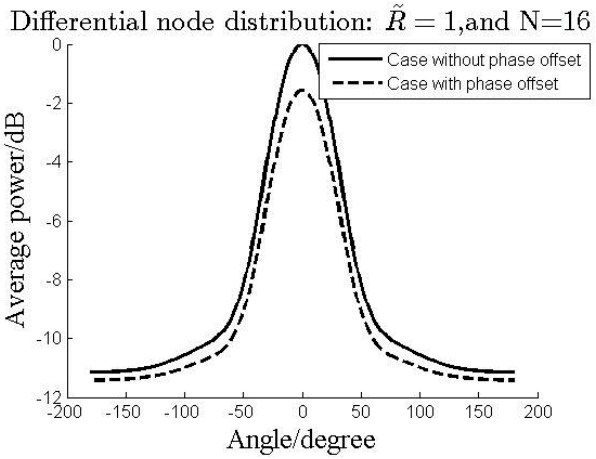

Fig. 7. Average beampattern comparison for differential node distribution.

The loop SNR for phase noise is set to be 5 dB in those figures. It can be seen that the degradation factor pulls down the array gain at the desired direction about 1.7 dB whereas the floor of the average beampattern remains unchanged at 10 log(1/16) = –12 dB.

The 3dB width, 3dB sidelobe region, normalized directivity and CCDF of the three node distributions for the cases with or without phase noise are shown in Figs. 8-11 respectively. Figs. 8-10 show that the beampattern properties of the case with phase noise will tend to those of the case without phase noise as the loop SNR increases, which matches the results in (11) and (12). Since the degradation factor pulls down the average beampattern in the whole region $\phi \in [-\pi, \pi)$, 3dB width, 3dB sidelobe region, and CCDF of the case with phase noise are smaller than those of the case without phase noise as shown in Figs. 8, 9, and 11. It can be seen from Figs. 5-7 that both of the mainlobe and sidelobe are affected by the degradation factor. However, Fig. 10 shows that the case with phase noise has smaller normalized directivity than the case without phase noise. This implies that the desired direction loses more power than the other directions. Fig. 5 and Figs. 8-10 also show that the estimated and theoretical beampattern properties are basically same for the case of uniform node distribution and Tikhonov phase noise model, which means the proposed method is effective.

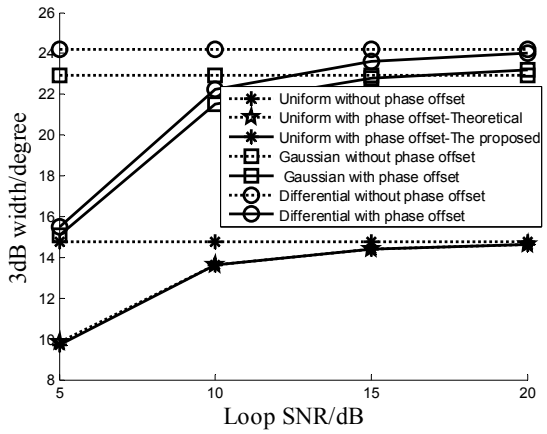

Fig. 8. 3dB width comparison.

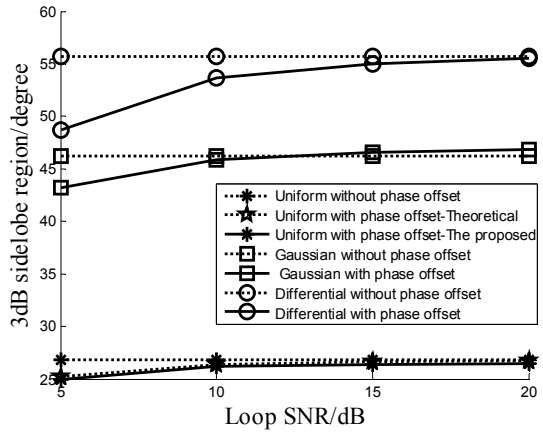

Fig. 9. 3dB sidelobe region comparison.

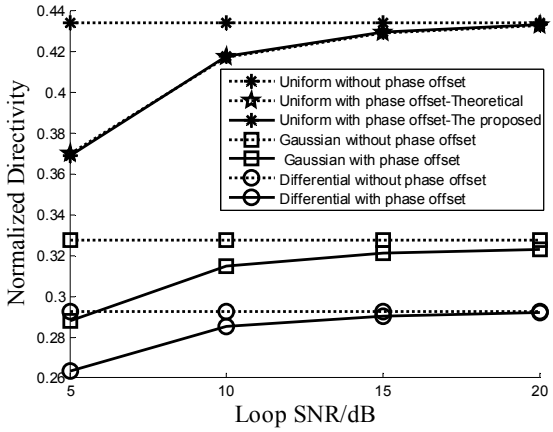

Fig. 10. Normalized directivity comparison.

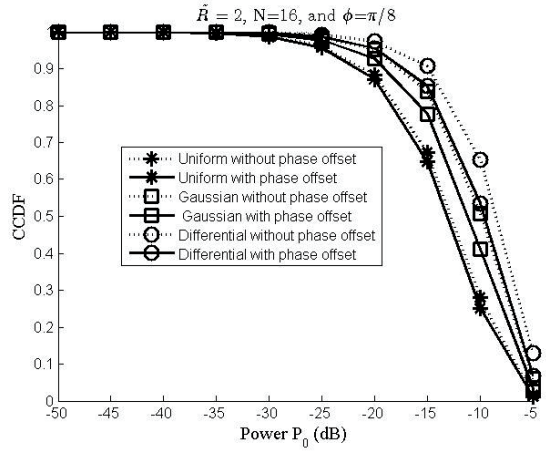

Fig. 11. CCDF comparison when the normalized radius is 2 and $\phi = \pi / 8$.

6. Conclusions

This paper proposes a unified method to evaluate the performance of collaborative beamforming with phase noise. Some characteristics of collaborative beamforming such as average beampattern, 3dB width, 3dB sidelobe region, average directivity, and CCDF are derived using the proposed method. Since the non-parametric kernel method is used to build the PDFs of node and phase offset

distributions, the proposed non-parametric approach can provide accurate performance analysis for various node and phase noise distributions which may or may not be represented by explicit PDF functions. The theoretical analysis and simulation results show that the proposed method is effective for arbitrary node distributions and any phase offset.

Appendix

A. Derivation of the average beampattern

Substituting (7), (8), and (9) into (10), gives:

$$\begin{aligned} P_{av}(\phi) &= \int_{-\infty}^{+\infty}\int_{-\infty}^{+\infty} P(\phi \mid \mathbf{z},\boldsymbol{\varphi}) f_{z_k}(\mathbf{z}) f_{\varphi_k}(\boldsymbol{\varphi}) d\mathbf{z} d\boldsymbol{\varphi} \\ &= \frac{1}{N} + \frac{1}{N^2}\sum_{k=1}^{N}\sum_{t=1}^{L}\int_{-\infty}^{+\infty} \frac{e^{j\varphi_k}}{\sqrt{2\pi}Ls}\exp\left(-\frac{(\varphi_k-\overline{\varphi}_t)^2}{2s^2}\right)d\varphi_k \\ &\cdot\sum_{t=1}^{M}\int_{-\infty}^{+\infty}\frac{e^{-jaz_k}}{\sqrt{2\pi}Mh}\exp\left(-\frac{(z_k-\overline{z}_t)^2}{2h^2}\right)dz_k \\ &\cdot\sum_{l=1,l\neq k}^{N}\sum_{t=1}^{L}\int_{-\infty}^{+\infty}\frac{e^{-j\varphi_l}}{\sqrt{2\pi}Ls}\exp\left(-\frac{(\varphi_l-\overline{\varphi}_t)^2}{2s^2}\right)d\varphi_l \\ &\cdot\sum_{t=1}^{M}\int_{-\infty}^{+\infty}\frac{e^{jaz_l}}{\sqrt{2\pi}Mh}\exp\left(-\frac{(z_l-\overline{z}_t)^2}{2h^2}\right)dz_l \end{aligned} \tag{29}$$

where

$$\begin{aligned} &\int_{-\infty}^{+\infty}\frac{e^{-jaz_k}}{\sqrt{2\pi}Mh}\exp\left(-\frac{(z_k-\overline{z}_t)^2}{2h^2}\right)dz_k \\ &= \frac{1}{M}\exp\left(\frac{(\overline{z}_t - jah^2)^2-\overline{z}_t^2}{2h^2}\right)\times \\ &\int_{-\infty}^{+\infty}\frac{1}{\sqrt{2\pi}h}\exp\left(-\frac{(z_k+(jah^2-\overline{z}_t))^2}{2h^2}\right)dz_k \\ &= \frac{1}{M}e^{-\frac{a^2h^2}{2}}e^{-ja\overline{z}_t} \\ &\int_{-\infty}^{+\infty}\frac{e^{jaz_l}}{\sqrt{2\pi}Mh}\exp\left(-\frac{(z_l-\overline{z}_t)^2}{2h^2}\right)dz_l \\ &= \frac{1}{M}e^{-\frac{a^2h^2}{2}}e^{ja\overline{z}_t} \\ &\int_{-\infty}^{+\infty}\frac{e^{j\varphi_k}}{\sqrt{2\pi}Ls}\exp\left(-\frac{(\varphi_k-\overline{\varphi}_t)^2}{2s^2}\right)d\varphi_k \\ &= \frac{1}{L}e^{-\frac{s^2}{2}}e^{j\overline{\varphi}_t} \\ &\int_{-\infty}^{+\infty}\frac{e^{-j\varphi_l}}{\sqrt{2\pi}Ls}\exp\left(-\frac{(\varphi_l-\overline{\varphi}_t)^2}{2s^2}\right) \\ &= \frac{1}{L}e^{-\frac{s^2}{2}}e^{-j\overline{\varphi}_t} \end{aligned} \tag{30}$$

Substituting (30) into (29), gives:

$$\begin{aligned} P_{av}(\phi) &= \frac{1}{N} + \frac{1}{N^2}\sum_{k=1}^{N}\sum_{t=1}^{L}\frac{1}{L}e^{-\frac{s^2}{2}}e^{j\overline{\varphi}_t}\sum_{t=1}^{M}\frac{1}{M}e^{-\frac{a^2h^2}{2}}e^{-ja\overline{z}_t} \\ &\cdot\sum_{l=1,l\neq k}^{N}\sum_{t=1}^{L}\frac{1}{L}e^{-\frac{s^2}{2}}e^{-j\overline{\varphi}_t}\sum_{t=1}^{M}\frac{1}{M}e^{-\frac{a^2h^2}{2}}e^{ja\overline{z}_t} \\ &= \frac{1}{N} + \left(1-\frac{1}{N}\right)e^{-s^2}e^{-a^2h^2}\left|A_\varphi\right|^2\left|A_z\right|^2 \end{aligned} \tag{31}$$

where $A_\varphi = \frac{1}{L}\sum_{t=1}^{L}e^{j\overline{\varphi}_t}$, and $A_z = \frac{1}{M}\sum_{t=1}^{M}e^{-ja\overline{z}_t}$.

Note that $h\to 0$, $s\to 0$ when $M\to\infty$, $L\to\infty$ [15]. When the sizes of survey sets M and L are large enough, $P_{av}(\phi)$ can be further simplified as:

$$P_{av}(\phi) = \frac{1}{N} + \left(1-\frac{1}{N}\right)\left|A_\varphi\right|^2\left|A_z\right|^2 \tag{32}$$

where $\left|A_\varphi\right|^2$ can be obtained from the survey set $\{\overline{\varphi}_1,\overline{\varphi}_2,\cdots,\overline{\varphi}_L\}$:

$$\begin{aligned} \left|A_\varphi\right|^2 &= A_\varphi A_\varphi^* \\ &= \frac{1}{L^2}\sum_{t_1=1}^{L}e^{j\overline{\varphi}_{t_1}}\sum_{t_2=1}^{L}e^{-j\overline{\varphi}_{t_2}} \\ &= \frac{1}{L} + \frac{1}{L^2}\sum_{t_1=1}^{L}e^{j\overline{\varphi}_{t_1}}\sum_{t_2\neq t_1,t_2=1}^{L}e^{-j\overline{\varphi}_{t_2}} \end{aligned} \tag{33}$$

B. **Proposition 1:** The average beampattern derived using the proposed method will become that of the Gaussian [8] or uniform [6] case when the nodes are subject to the corresponding distribution and phase offset tends to 0.

Proof: In the case of the perfect phase synchronization, the proposed average beampattern (11) reduces to (12) and equation (12) can be rewritten as:

$$P_{av}(\phi) = \frac{1}{N} + \left(1-\frac{1}{N}\right)\left(\left(\frac{1}{M} + \frac{1}{M^2}\sum_{t_1=1}^{M}e^{-ja\overline{z}_{t_1}}\sum_{t_2=1,t_1\neq t_2}^{M}e^{-ja\overline{z}_{t_2}}\right)\right). \tag{34}$$

Since $\overline{z}_t$ is a random variable, the proposed average beampattern $P_{av}(\phi)$ for Gaussian case becomes:

$$\begin{aligned} P_{av}(\phi) &= \frac{1}{N} + \left(1-\frac{1}{N}\right)\left(\frac{1}{M} + \frac{1}{M^2}\sum_{t_1=1}^{M}\int_{-\infty}^{+\infty}e^{-ja\overline{z}_{t_1}}\frac{1}{\sqrt{2\pi}\sigma}\right. \\ &\left.\cdot e^{-\frac{\overline{z}_{t_1}^2}{2\sigma^2}}d\overline{z}_{t_1}\sum_{t_2=1,t_1\neq t_2}^{M}\int_{-\infty}^{+\infty}e^{-ja\overline{z}_{t_2}}\frac{1}{\sqrt{2\pi}\sigma}e^{-\frac{\overline{z}_{t_2}^2}{2\sigma^2}}d\overline{z}_{t_2}\right) \\ &= \frac{1}{N} + \left(1-\frac{1}{N}\right)\left(\frac{1}{M} + \left(1-\frac{1}{M}\right)\left|e^{-\frac{a^2\sigma^2}{2}}\right|^2\right) \end{aligned} \tag{35}$$

where σ^2 is the variance of the Gaussian distribution. As $M\to\infty$, the proposed average beampattern for Gaussian case becomes:

$$P_{av}(\phi) = \frac{1}{N} + \left(1 - \frac{1}{N}\right)\left|e^{-\frac{a^2\sigma^2}{2}}\right|^2 . \quad (36)$$

Equation (36) shows that the average beampattern derived using the proposed method will become the Gaussian average beampattern in [8] when the nodes are subject to the Gaussian distribution and phase offset tends to 0. The relationship between the proposed average beampattern and uniform average beampattern in [6] has the similar conclusion.

Acknowledgements

This work was supported by the Open Research Fund of The Academy of Satellite Application under grant (2012-1518), the National Natural Science Foundation of China (61201275 and 61101094), China Postdoctoral Science Foundation (2013M540532), and Jiangxi Postdoctoral Research Project (2013KY01).

References

[1] AKYILDIZ, I. F., WEILIAN, SU, SANKARASUBRAMANIAM, Y., CAYIRCI, E. A survey on sensor networks. *IEEE Commun. Mag.,* Aug. 2002, vol. 40, no. 8, p. 102–114.

[2] MUDUMBAI, R., BARRIAC, G., MADHOW, U. On the feasibility of distributed beamforming in wireless networks. *IEEE Trans. Wireless Commun.,* May 2007, vol. 6, no. 5, p. 1754-1763.

[3] MAN-ON, PUN, BROWN, D. R., POOR, H. V. Opportunistic collaborative beamforming with one-bit feedback. *IEEE Trans. Wireless Commun.,* May 2009, vol. 8, no. 5, p. 2629-2641.

[4] NOURI, N., NOORI, N. Directional relays for multi-hop cooperative cognitive radio networks. *Radioengineering*, Sep. 2013, vol. 22, no. 3, p. 791-799.

[5] PFEFFER, C., SCHEIBLHOFER, S., FEGER, R., STELZER, A. An S-FSCW based multi-channel reader system for beamforming applications using surface acoustic wave sensors. *Radioengineering*, Dec 2011, vol. 20, no. 4, p. 745-751.

[6] OCHIAI, H., MITRAN, P., POOR, H. V., TAROKH, V. Collaborative beamforming for distributed wireless ad hoc sensor networks. *IEEE Trans. Signal Processing,* Nov. 2005, vol. 53, no. 11, p. 4110-4124.

[7] LO, Y. T. A mathematical theory of antenna arrays with randomly spaced elements. *IEEE Trans. Antennas Propag.,* May 1964, vol. 12, no. 3, p. 257-268.

[8] AHMED, M. F. A., VOROBYOV, S. A. Collaborative beamforming for wireless sensor networks with Gaussian distributed sensor nodes. *IEEE Trans. Wireless Commun.,* Feb. 2009, vol. 8, no. 2, p. 638-643.

[9] HUANG, J. Y., WANG P., WAN, Q. Collaborative beamforming for wireless sensor networks with arbitrary distributed sensors. *IEEE Communications Letters,* July 2012, vol. 16, no. 7, p. 1118 to 1120.

[10] PLATANIOTIS, K. N., ANDROUTSOS, D., VINAYAGAMOORTHY, S., VENETSANOPOULOS, A. N. Color image processing using adaptive multichannel filters. *IEEE Trans. Image Processing,* July 1997, vol. 6, no. 7. p. 933–949.

[11] ELGAMMAL, A., DURAISWAMI, R., HARWOOD, D., DAVIS, L. S. Background and foreground modeling using nonparametric kernel density estimation for visual surveillance. *Proceedings of the IEEE,* Jul. 2002, vol. 90, no. 7, p. 1151-1163.

[12] WANG, D. M., CHENG, Y., WANG, Y., AGRAWAL, D. P. Lifetime enhancement of wireless sensor networks by differentiable node density deployment. In *IEEE International Conference on Mobile Adhoc and Sensor Systems (MASS).* 2006, p. 546-549.

[13] HAN, T. S., HOSHI, M. Interval algorithm for random number generation. *IEEE Trans. Inf. Theory*, 1997, vol. 43, no. 2, p. 599–611.

[14] KNUTH, D., YAO, A. The complexity of nonuniform random number generation. In *Algorithms Complex.: New Directions and Recent Results*, 1976, p. 357–428.

[15] DE LA ROSA, J. I., FLEURY, G. A., DAVOUST, M. E. Minimum-entropy, PDF approximation, and kernel selection for measurement estimation. *IEEE Trans. Instrumentation and Measurement,* Aug. 2003, vol. 52, no. 4, p. 1009-1020.

About Authors …

Xiaofeng SHEN was born in 1969. He received the B.Eng degree from the Zhejiang University, Hangzhou, China, in 1990, the M.Eng. from the University of Electronic Science and Technology of China, Chengdu, China, in 1996. Currently, he is an associate professor at the University of Electronic Science and Technology of China.

Jiyan HUANG was born in Jiangxi, China, on 05, Sep, 1981. He received the B.Eng (Hons.), M.Eng., and Ph.D. degrees from the University of Electronic Science and Technology of China (UESTC), Chengdu, China, in 2003, 2005, and 2008, respectively. Currently, he is an associate professor at the University of Electronic Science and Technology of China.